Electronic Supplementary Material (ESI) for ChemComm.
This journal is © The Royal Society of Chemistry 2017

Supporting Information

Tri- and Hexaferrocenyl- Substituted Subphthalocyanines in Quest for the Optimum Electron Donor-Acceptor Distance

Javier Fernández-Ariza,[a] Rafael M. Krick Calderón,[b] Josefina Perles, [c] M. Salomé Rodríguez-Morgade,*[,a,d] Dirk M. Guldi*[,b] and Tomás Torres*[,a,d,e]

[a] *Departamento de Química Orgánica, Universidad Autónoma de Madrid, Cantoblanco, 28049 Madrid, Spain. E-mail: tomas.torres@uam.es, salome.rodriguez@uam.es*

[b] *Department of Chemistry and Pharmacy & Interdisciplinary Center for Molecular Materials (ICMM), University of Erlangen-Nuremberg, Egerlandstraße 3, 91058 Erlangen, (Germany)E-mail: dirk.guldi@fau.de.*

[c] *Laboratorio de DRX Monocristal, Servicio Interdepartamental de Investigación, Universidad Autónoma de Madrid (UAM), Cantoblanco, 28049 Madrid, Spain*

[d]*Institute for Advanced Research in Chemical Sciences (IAdChem), Universidad Autónoma de Madrid, 28049 Madrid, Spain.*

[e] *Instituto Madrileño de Estudios Avanzados (IMDEA)-Nanocienciac/ Faraday, 9, Cantoblanco, 28049 Madrid, Spain*

Contents

1. General Methods

Synthesis and Characterization. UV-vis spectra were recorded with a JASCO V-660. MALDI-TOF-MS spectra were obtained from a BRUKER ULTRAFLEX III instrument equipped with a nitrogen laser operating at 337 nm. NMR spectra were recorded with a BRUKER AC-300 (300 MHz) instrument. The temperature was actively controlled at 298 K. Chemical shifts are measured in ppm relative to the correspondent deuterated solvent. Carbon chemical shifts are measured downfield from TMS using the resonance of the deuterated solvent as the internal standard. Column chromatography was carried out on silica gel Merck-60 (230-400 mesh, 60 Å), and TLC on aluminium sheets pre-coated with silica gel 60 F254 (E. Merck). Infrared spectra (IR) were recorded on a Bruker Vector 22. Electrochemical measurements were performed on an Autolab PGStat 30 equipment using a three electrode configuration system. The measurements were carried out using DCM solutions containing 0.1 M tetrabutylammonium hexafluorophosphate ($TBAPF_6$). A glassy carbon electrode (3 mm diameter) was used as the working electrode, and a platinum wire and an Ag/AgNO3 (in CH_3CN) electrode were employed as the counter and the reference electrodes, respectively. Ferrocene (Fc) was used as an external reference and all the potentials were given relative to the Fc/Fc^+ couple. Femtosecond transient absorption studies were performed with 550 nm laser pulses (1 kHz, 150 fs pulse width, 150 nJ) from an amplified Ti/sapphire laser system (Model CPA 2101, Clark-MXR Inc. – output 775 nm).

Computational methods: The Gaussian 09 software package[i] was used to carry out DFT calculations using the B3LYP functional with 6-31G(d,p) basis set. Structural optimization was performed on model compounds of **1** and **3** based on the crystal structure of **3** with the six ferrocenyl substituents and also by replacing three of them with hydrogen atoms.

Starting Materials. Chemicals were purchased from commercial suppliers and used without further purification. Solid, hygroscopic reagents were dried in a vacuum oven before use. Reaction solvents were thoroughly dried before use using standard methods. The syntheses and characterization of the starting SubPcs **2**[ii] and SubPc **5**[iii] have been previously reported.

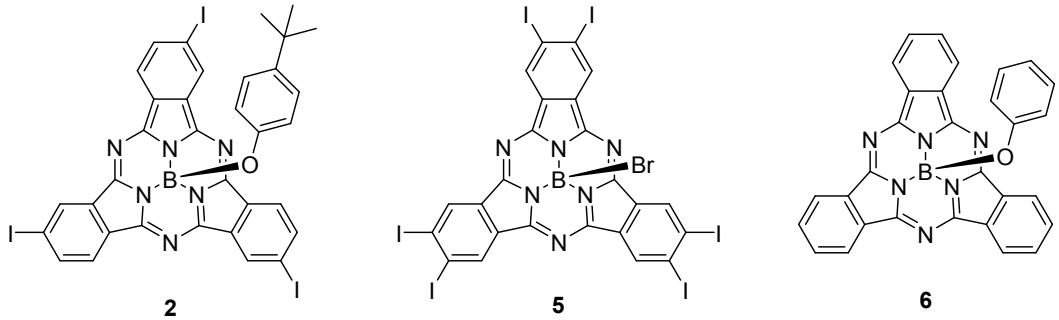

Chart S1. Structures of SubPc precursors **2** and **5** and SubPc reference **6**.

2. Synthetic procedures and characterization data of compounds 1, 3 and 4

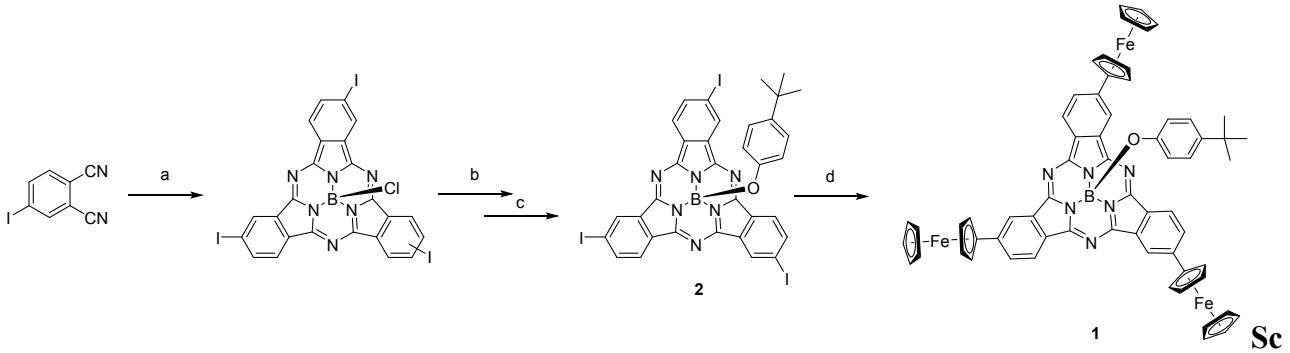

Scheme S1. Synthesis of Fc_3SubPc **1**. a) BCl_3 (*p*-xylene), 140ºC; b) 4-(*tert*-butyl)phenol, toluene, reflux; c) Separation of regioisomers by column chromatography; d) $FcB(OH)_2$, $Pd(dppf)Cl_2$, Cs_2CO_3, toluene/water, reflux.

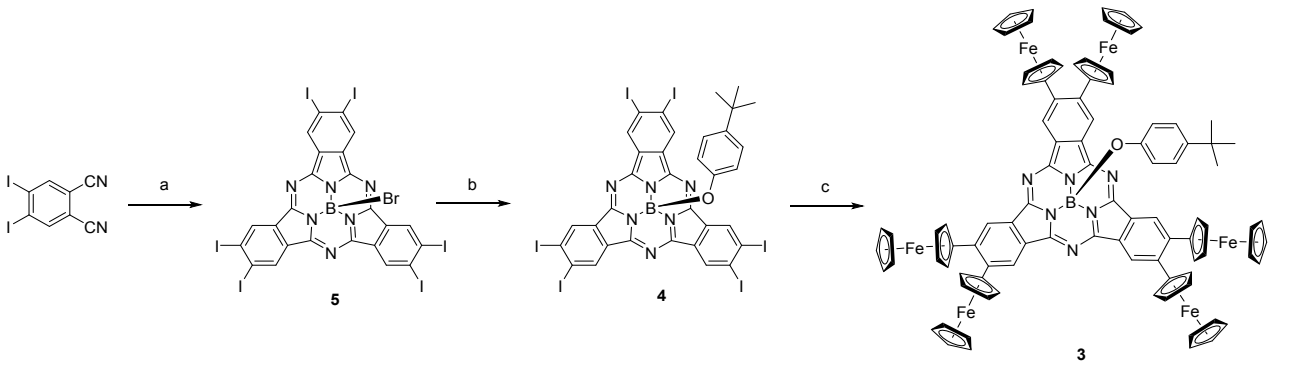

Scheme S2. Synthesis of Fc_6SubPc **3**.a) BBr_3, chlorobenzene/THF, 60ºC; b) 4-(*tert*-butyl)phenol, toluene/THF, reflux; c) $FcB(OH)_2$, $Pd(dppf)Cl_2$, Cs_2CO_3, toluene/water, reflux.

2.1 Fc_3SubPc 1[iv]

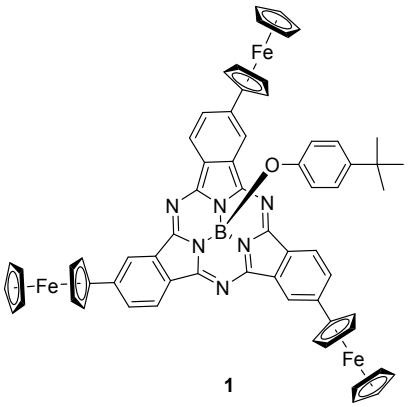

1

A 50 mL Schlenk flask was charged with C_3-triiodosubphthalocyanine (**2**) (50 mg, 0.054 mmol), ferrocenylboronic acid (41 mg, 0.179 mmol), $Pd(dppf)Cl_2$ (8.2 mg, 0.01 mmol), Cs_2CO_3 (0.53 g, 1.63 mmol), toluene (4 mL) and H_2O (4 mL). The resulting solution was deoxygenated *via* three Freeze-Pump-Thaw cycles and refluxed for 2h under argon atmosphere. The organic phase was separated, washed with brine, dried over $MgSO_4$ and then, evaporated till dryness. The crude product was purified by filtration on a silica gel plug (eluent: $CHCl_3$) to give 36 mg of **1** (60%) as a purple solid.

^{1}H NMR (300 MHz, $CDCl_3$): δ (ppm) = 8.89 (s, 3H), 8.77 (d, J_o = 8.3 Hz, 3H), 8.02 (dd, J_o = 8.4, J_m = 1.5 Hz, 3H), 6.80 (d, J_o' = 8.7 Hz, 2H), 5.39 (d, J_o' = 8.7 Hz, 2H), 4.98-4.94 (d, 6H), 4.49 (s, 6H), 4.08 (s, 14H), 1.09 (s, 9H).

^{13}C NMR (75.5 MHz, $CDCl_3$): δ (ppm) = 151.61, 151.55, 150.53, 143.50, 142.75, 131.83, 128.66, 127.91, 125.84, 122.10, 118.69, 117.72, 84.39, 70.20, 70.16, 70.09, 67.43, 67.12, 33.97, 31.49.

MS (MALDI-TOF, DCTB): *m/z* = 1096

HRMS ($C_{64}H_{49}BFe_3N_6O$) $[M]^+$: Calculated: 1096.2119; Found: 1096.2105.

UV-vis (toluene): λ_{max} (nm) (log ε (dm^3 mol^{-1} cm^{-1})) = 605 (4.76), 555 (sh), 344 (4.53).

UV-vis ($CHCl_3$): λ_{max} (nm) (log ε (dm^3 mol^{-1} cm^{-1})) = 605 (4.76), 555 (sh), 346 (4.58), 323 (4.57), 275 (4.82).

FT-IR (KBr), ν (cm^{-1}): 3092, 2922, 2852, 2459, 2361, 2342, 1617, 1542, 1513, 1453, 1426, 1374, 1289, 1250, 1166, 1106, 1056, 941, 891, 817, 761, 733, 707, 644, 619, 449.

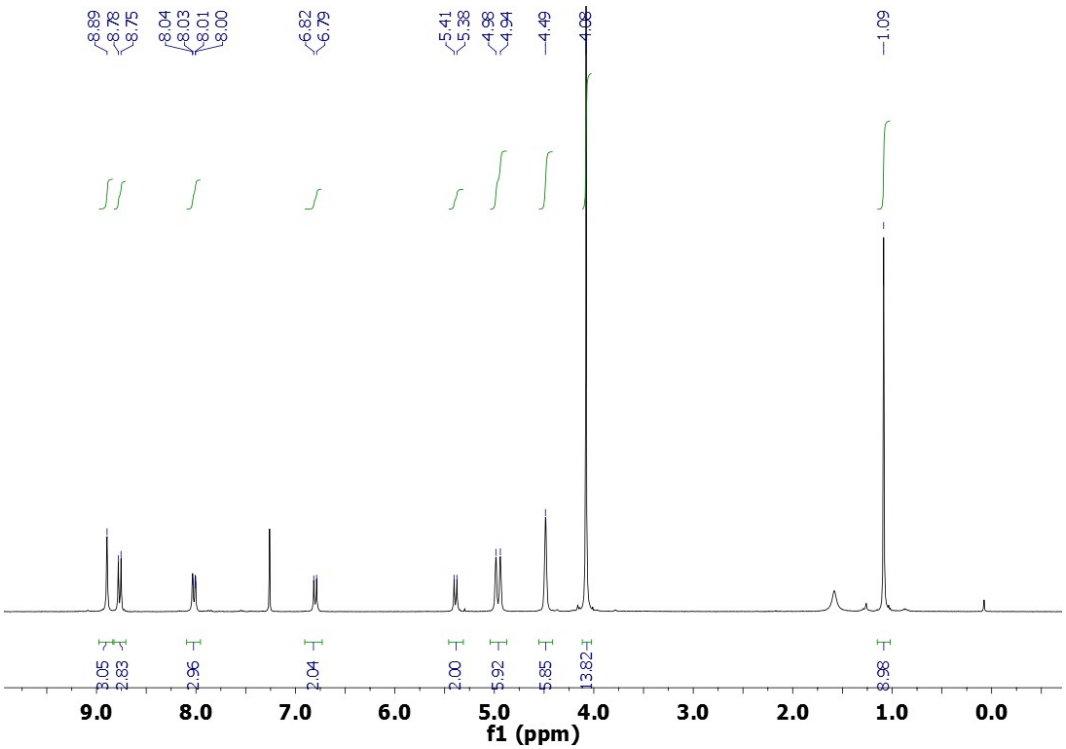

Figure S1. ^{1}H NMR (300 MHz, $CDCl_3$) of **1**

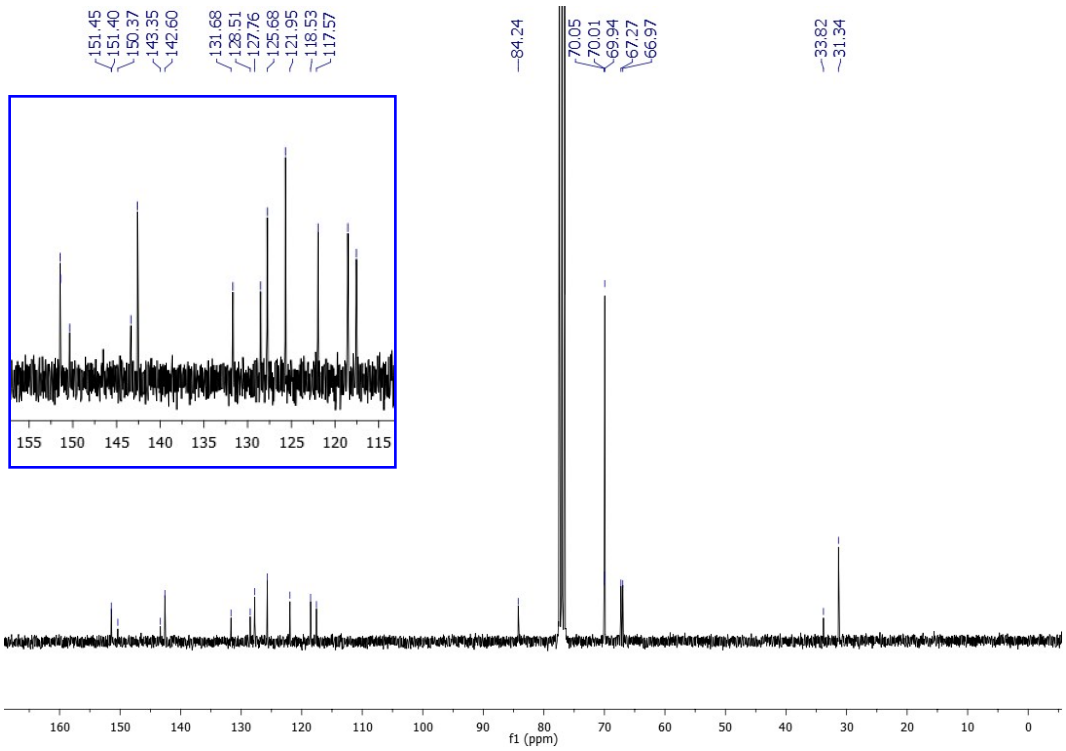

Figure S2. ^{13}C NMR (75.5 MHz, $CDCl_3$) of **1**

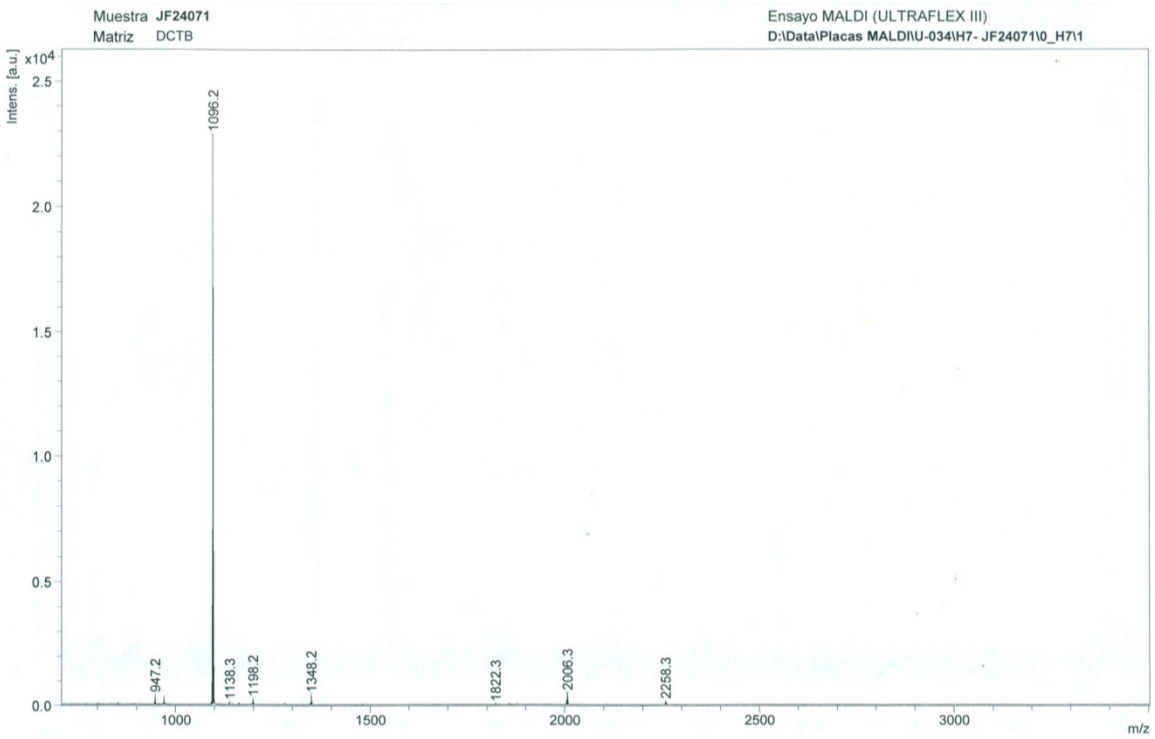

Figure S3. MS (MALDI-TOF, DCTB) of **1**.

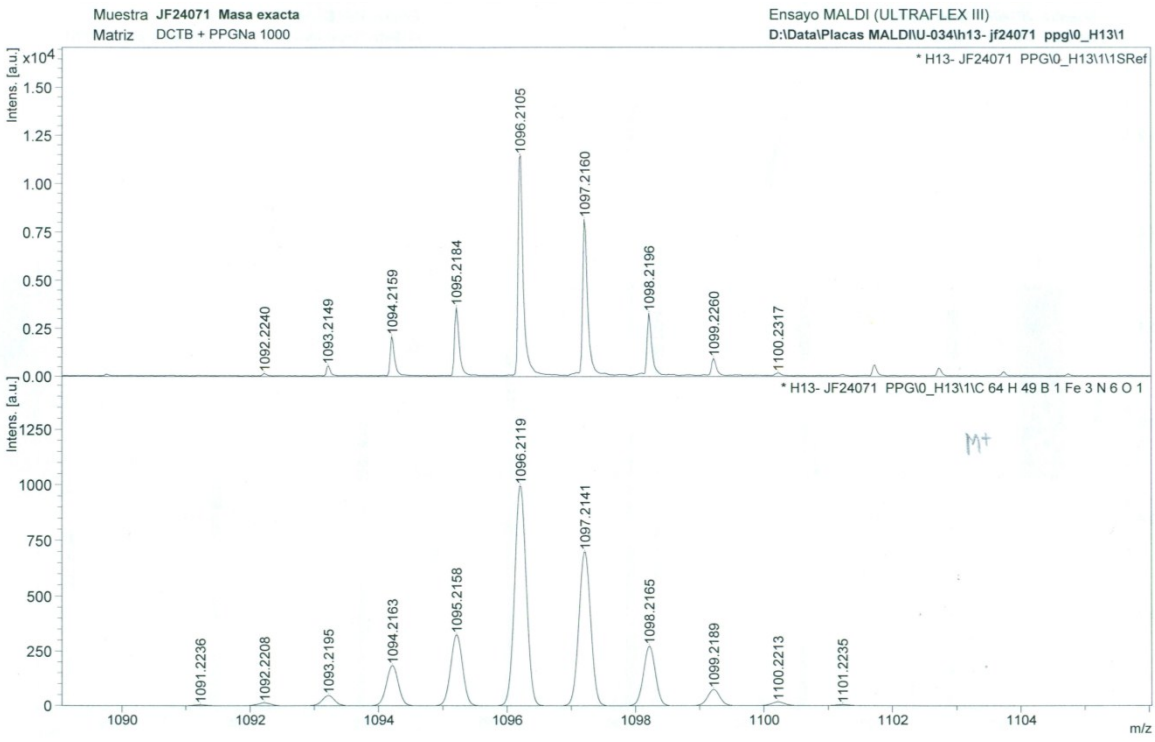

Figure S4. HRMS (MALDI-TOF, DCTB) of **1**. Bottom shows predicted isotopic pattern.

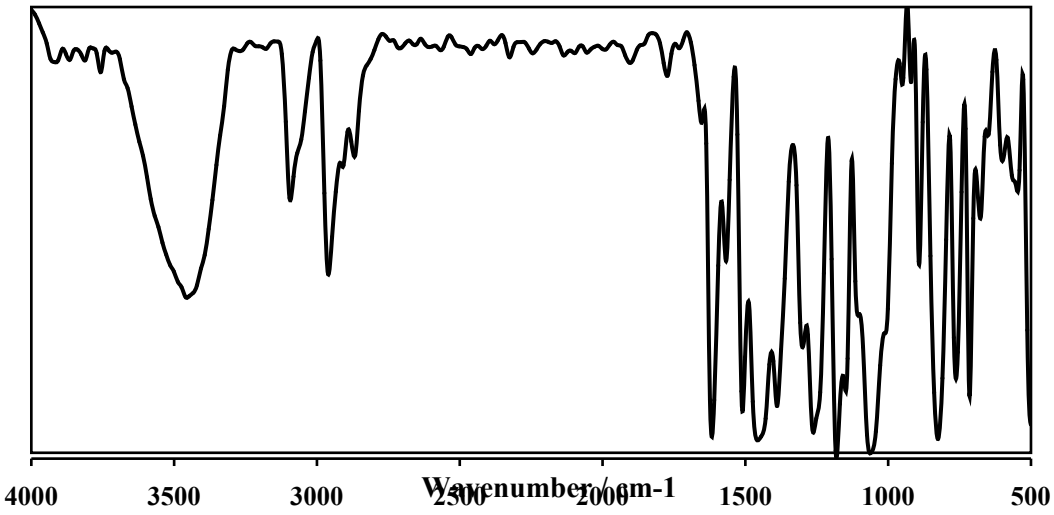

Figure S5. FT-IR (KBr) of **1**

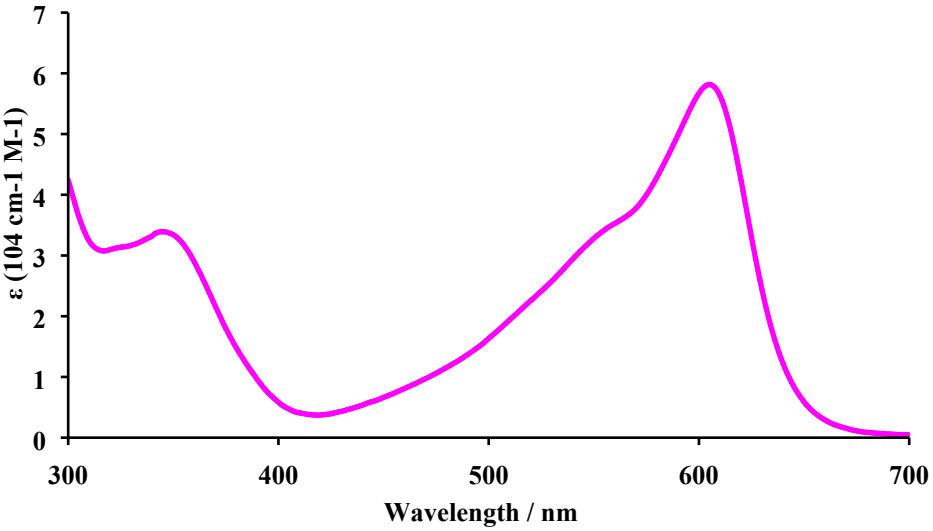

Figure S6. UV-vis (toluene) of **1.**

2.2 I_6SubPc 4

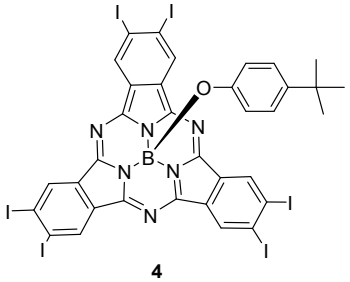

4

The crude hexaiodosubphthalocyanine **5** obtained from 4,5-diiodophthalonitrile (785 mg, 2 mmol) was dissolved with *tert*-butylphenol (3.1 g, 20 mmol) in a dry and degassed THF/toluene 1:1 mixture (4 mL). The solution was refluxed for 16 h. After cooling down to room temperature, the solvent was evaporated under reduced pressure and the resulting purple solid was washed with methanol. Purification by column chromatography on silica gel, using a (3:2) mixture of toluene/hexane as eluent, afforded SubPc **4** as a purple solid (105 mg, 12% overall).

^{1}H NMR (300 MHz, $CDCl_3$): δ (ppm) = 9.31 (s, 6H), 6.76 (m, J_o = 8.7 Hz, 2H), 5.25 (m, J_o = 8.7 Hz, 2H), 1.09 (s, 9H).

^{13}C NMR (75.5 MHz, $CDCl_3$): δ (ppm) = 150.14, 149.31, 132.64, 130.98, 125.87, 122.95, 117.81, 109.91, 33.88, 31.29.

MS (MALDI-TOF, DCTB): *m/z* = 1299.6 $[M]^+$.

HRMS: *m/z* Calcd for $[C_{34}H_{19}BI_6N_6O]$: 1299.5982; Found: 1299.5978

UV-vis (toluene): λ_{max} (nm) (log ε (dm^3 mol^{-1} cm^{-1})) = 583 (4.61), 561 (sh), 540 (4.13), 341 (4.22).

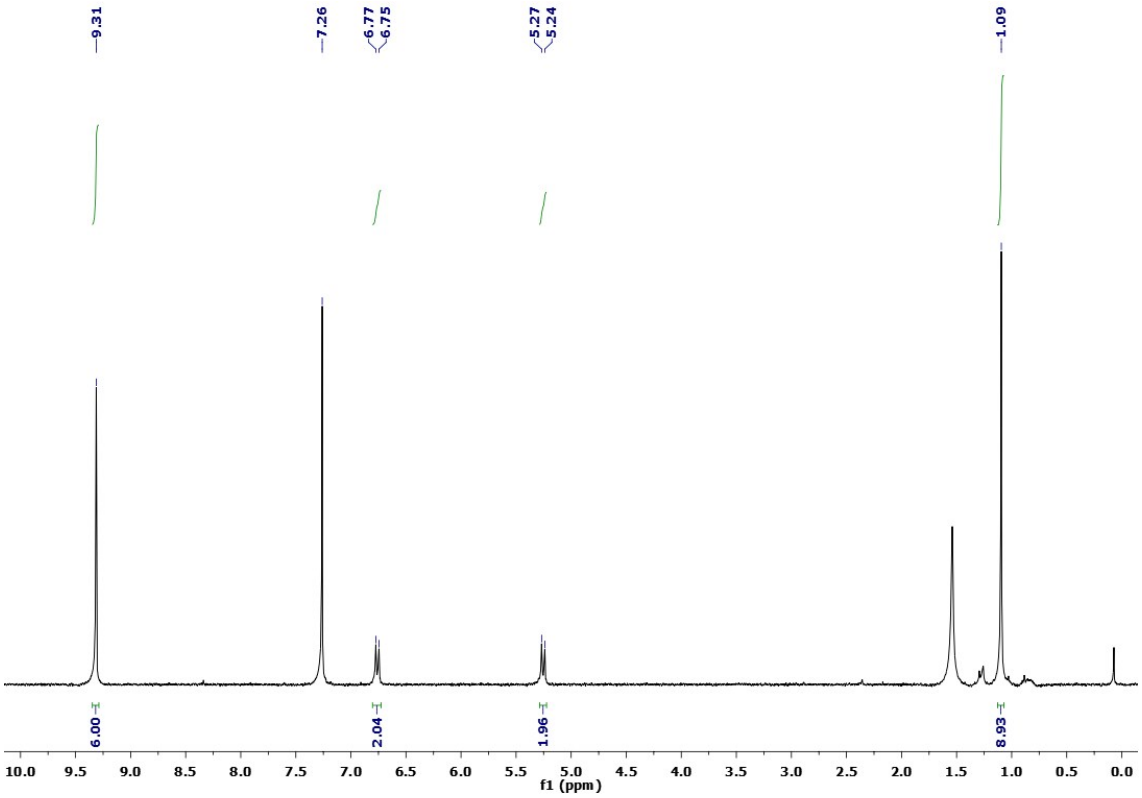

Figure S7. ^{1}H NMR (300 MHz, $CDCl_3$) of **4**

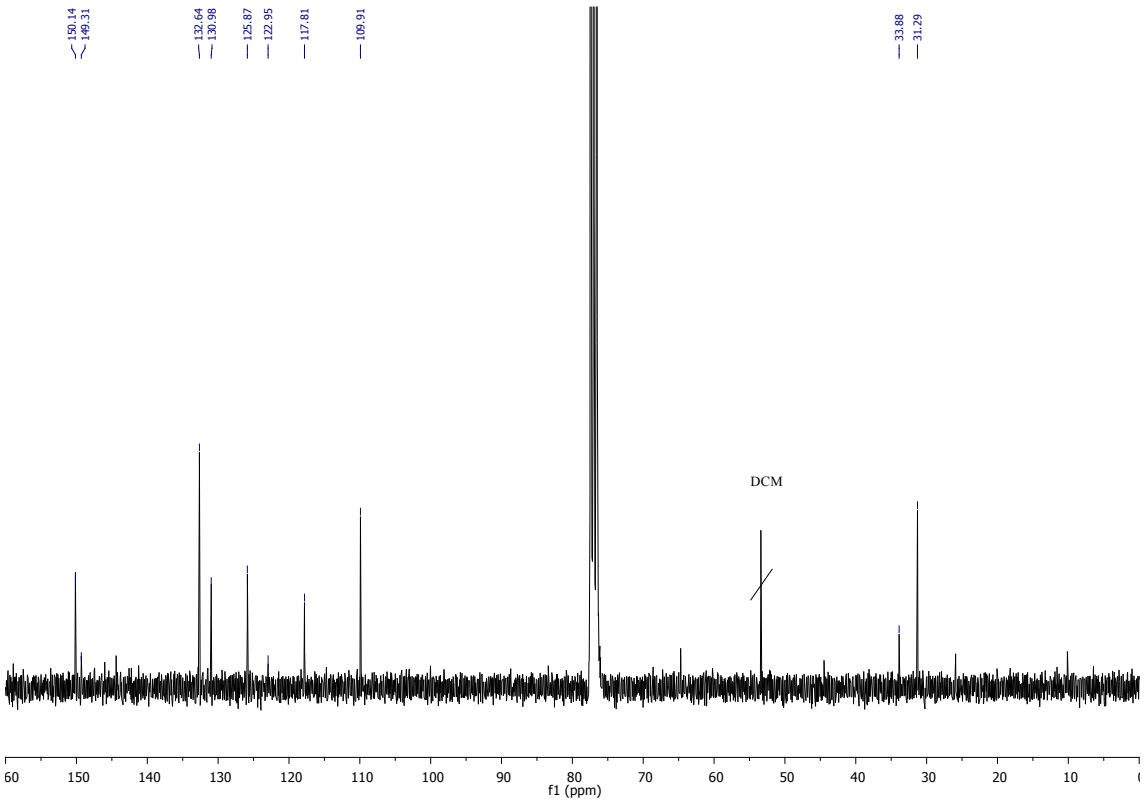

Figure S8. ^{13}C NMR (75.5 MHz, $CDCl_3$) of **4**

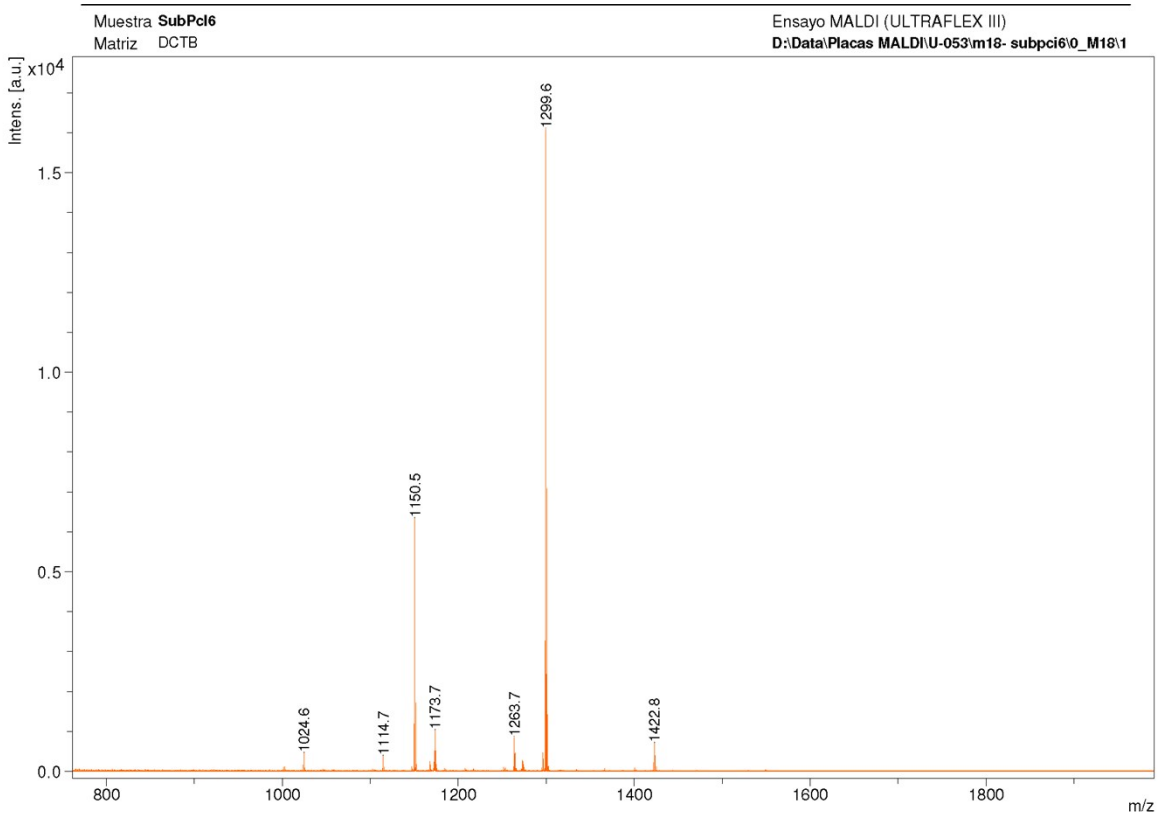

Figure S9. MS (MALDI-TOF, DCTB) of **4**

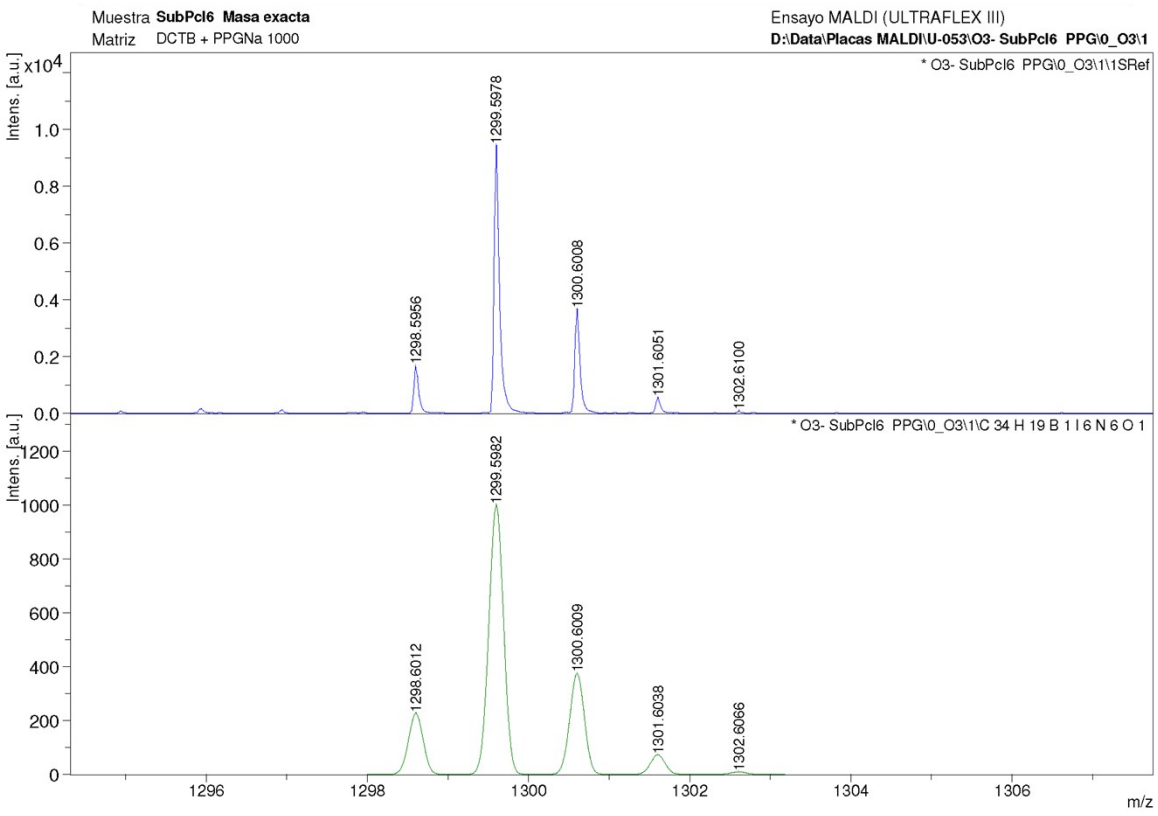

Figure S10. HRMS (MALDI-TOF, DCTB) of **4**. Bottom shows predicted isotopic pattern.

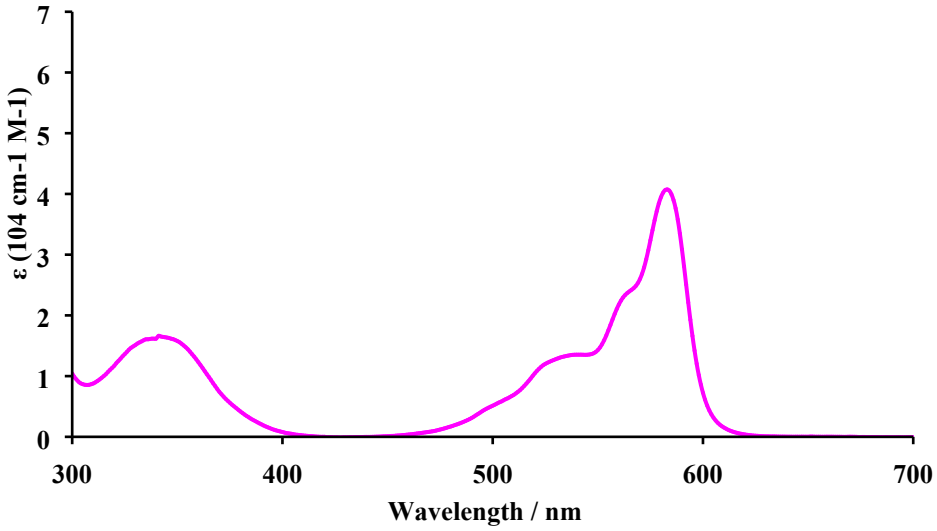

Figure S11. UV-vis (toluene) of **4**

2.3 Fc_6SubPc 3

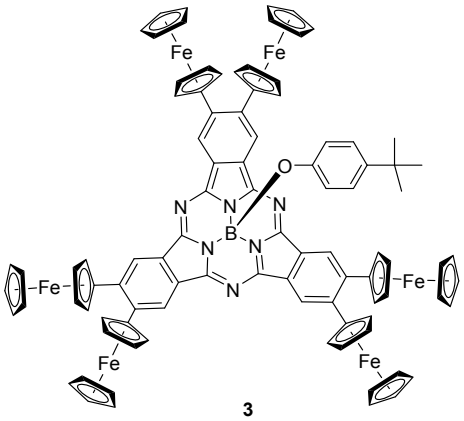

3

A 50 mL Schlenk flask was charged with hexaiodosubphthalocyanine **4** (50 mg, 0.038 mmol), ferrocenylboronic acid (58.3 mg, 0.254 mmol), $Pd(dppf)Cl_2$ (8.2 mg, 0.01 mmol), Cs_2CO_3 (0.38 g, 1.15 mmol), toluene (4 mL) and H_2O (4 mL). The resulting solution was deoxygenated *via* three Freeze-Pump-Thaw cycles and refluxed for 2h under argon atmosphere. The organic phase was separated, washed with brine, dried over $MgSO_4$ and then, evaporated until dryness. The crude product was chromatographed on silica gel (eluent: CH_2Cl_2/Hexane 1:1) to give 18 mg (28%) of **3** as a purple solid.

^{1}H NMR (300 MHz, $CDCl_3$): δ (ppm) = 9.23 (s, 6H), 6.88 (d, J_o = 8.6 Hz, 2H), 5.55 (d, J_o = 8.5 Hz, 2H), 4.62 – 3.87 (m, 54H), 1.12 (s, 9H).

^{13}C NMR (75.5 MHz, $CDCl_3$): δ (ppm) = 151.39, 140.49, 128.48, 125.79, 124.26, 117.84, 87.53, 71.36, 71.21, 69.85, 67.97, 31.40.

MS (MALDI-TOF, DCTB): *m/z* = 1649.

HRMS: *m/z* Calcd for $[C_{94}H_{73}BFe_6N_6O]$: 1648.2063; Found: 1648.2017

UV-vis (toluene): λ_{max} (nm) (log ε (dm^3 mol^{-1} cm^{-1})) = 632 (4.64), 576 (sh), 360 (sh), 341 (4.49).

UV-vis ($CHCl_3$): λ_{max} (nm) (log ε (dm^3 mol^{-1} cm^{-1})) = 631 (4.76), 572 (sh), 361 (sh), 340 (4.64), 273 (4.96).

FT-IR (KBr), ν (cm^{-1}): 3092, 2922, 2852, 2459, 2361, 1617, 1542, 1513, 1453, 1426, 1374, 1289, 1250, 1166, 1106, 1106, 1056, 941, 891, 817, 761, 733, 707, 644, 619, 449.

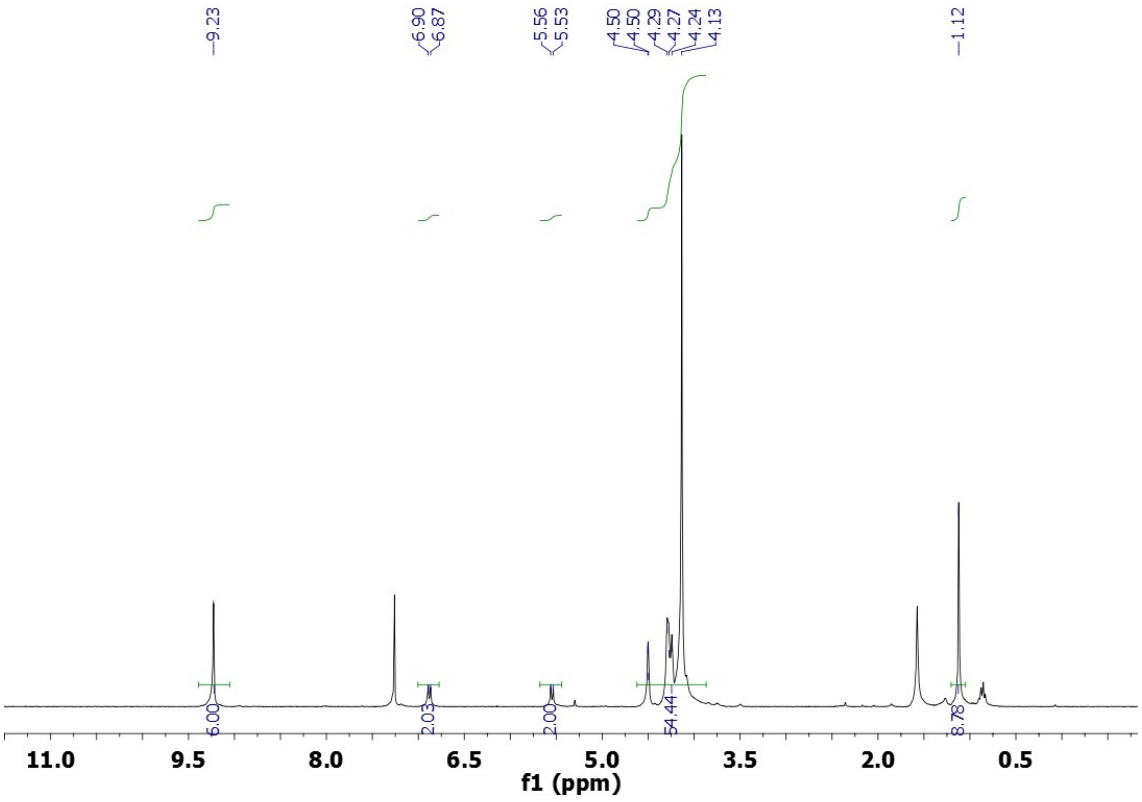

Figure S12. ^{1}H NMR (300 MHz, $CDCl_3$) of **3**

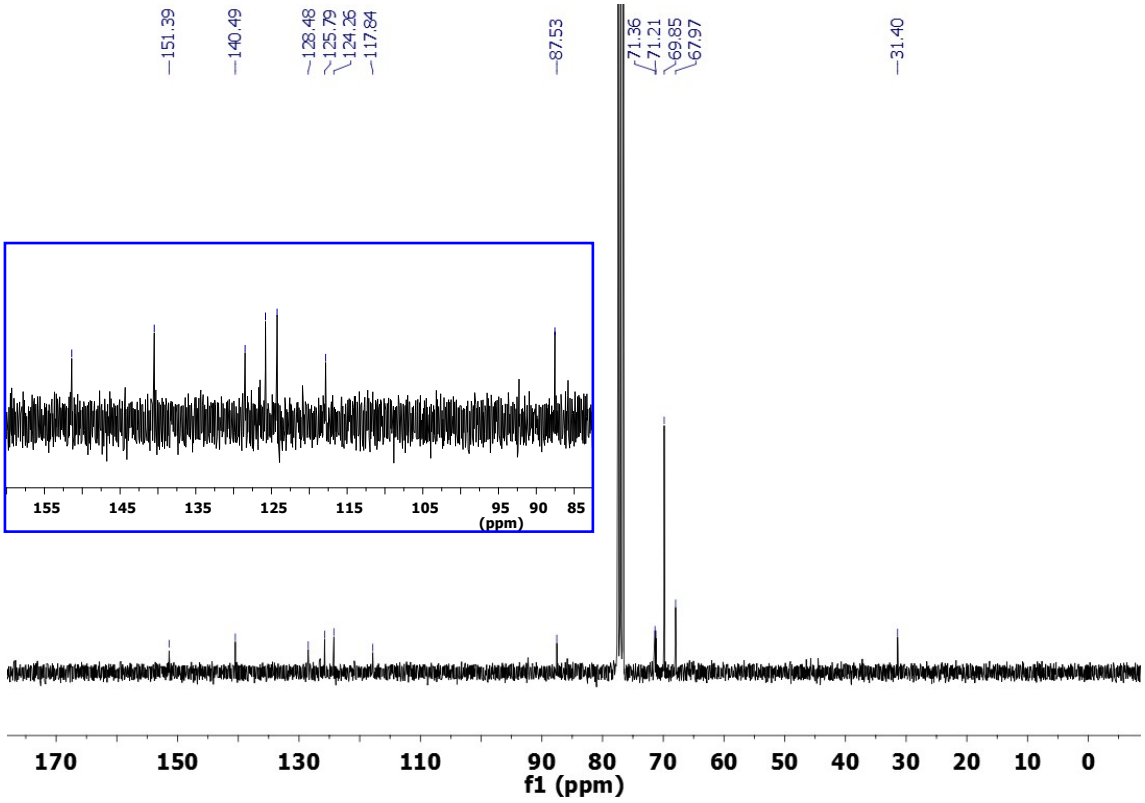

Figure S13. ^{13}C NMR (75.5 MHz, $CDCl_3$) of **3**

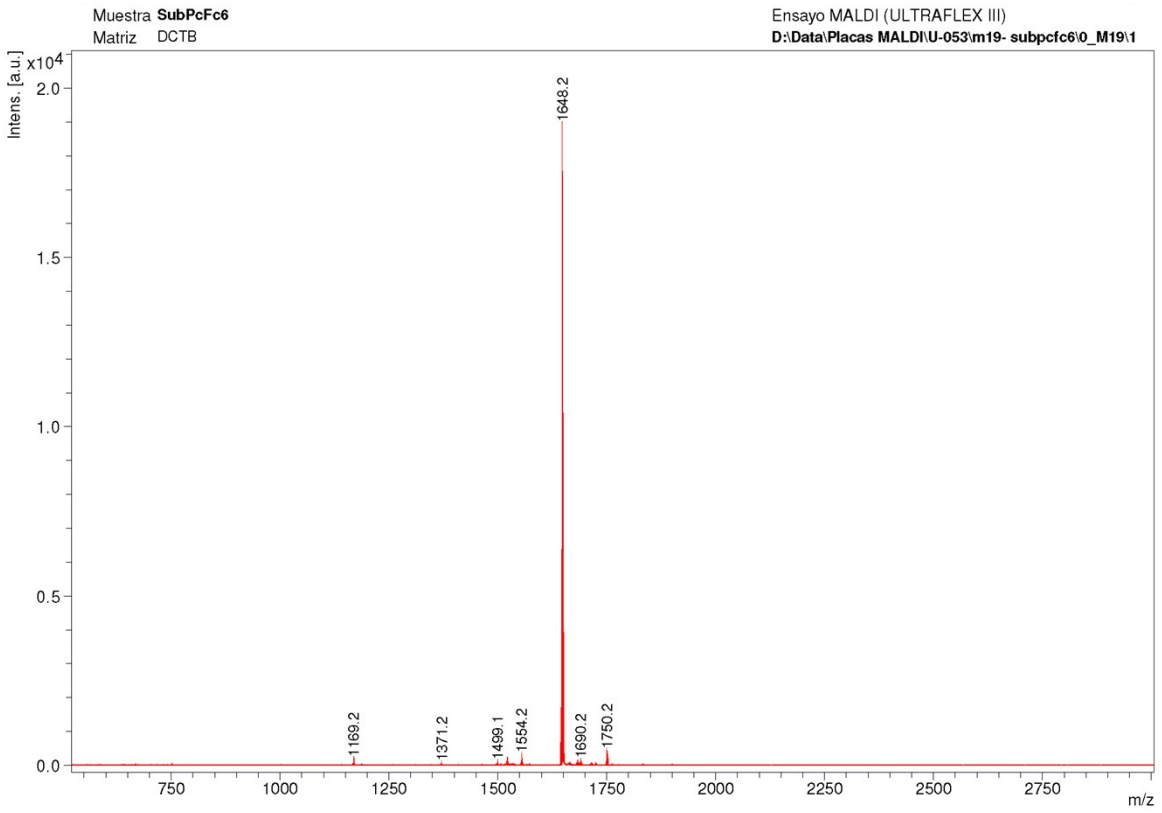

Figure S14. MS (MALDI-TOF, DCTB) of **3**

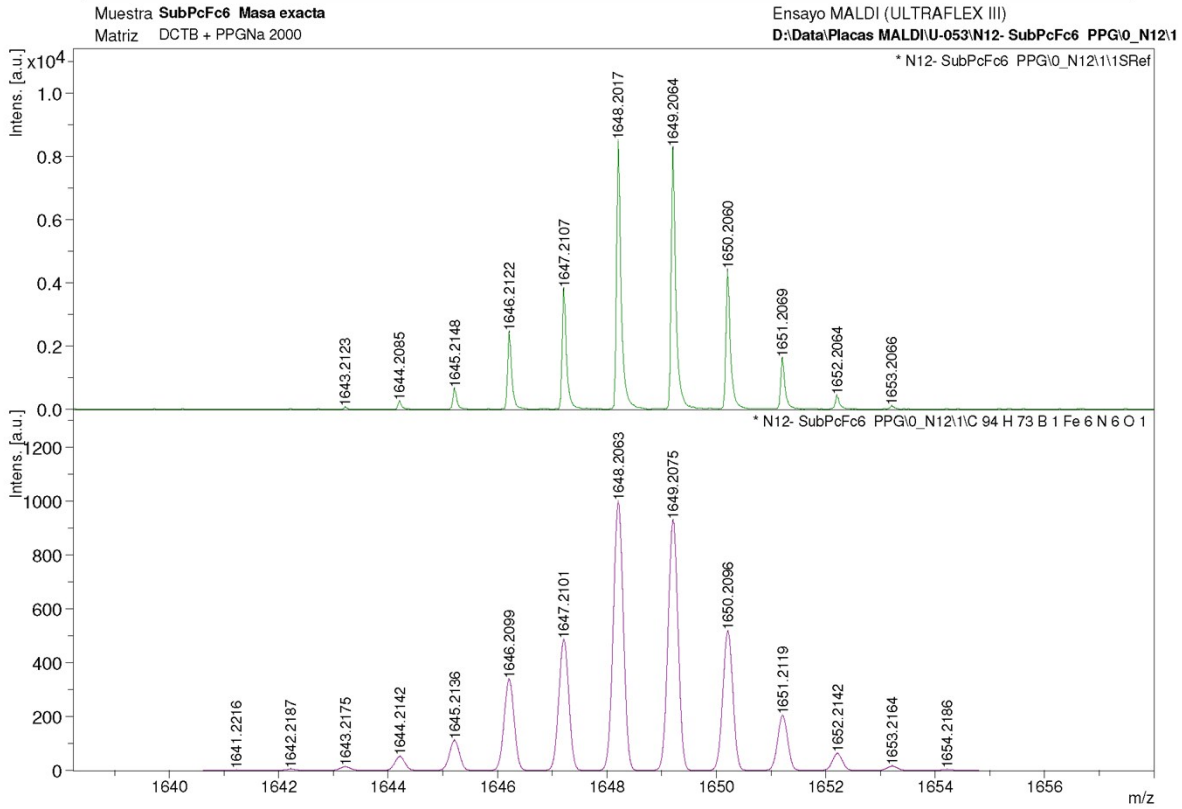

Figure S15. HRMS (MALDI-TOF, DCTB) of **3**. Enlargement showing the isotopic pattern.

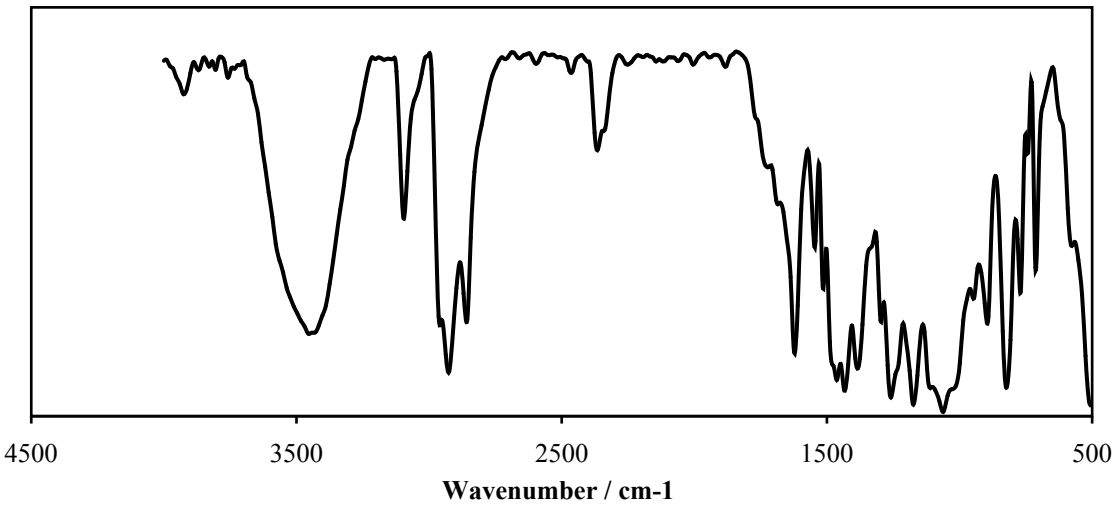

Figure S16. FT-IR spectrum (KBr) of **3**

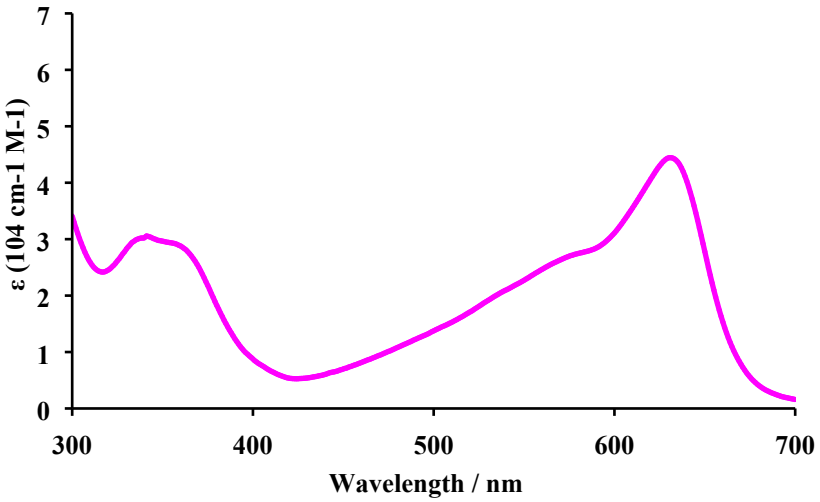

Figure S17. UV-vis spectrum (toluene) of **3**

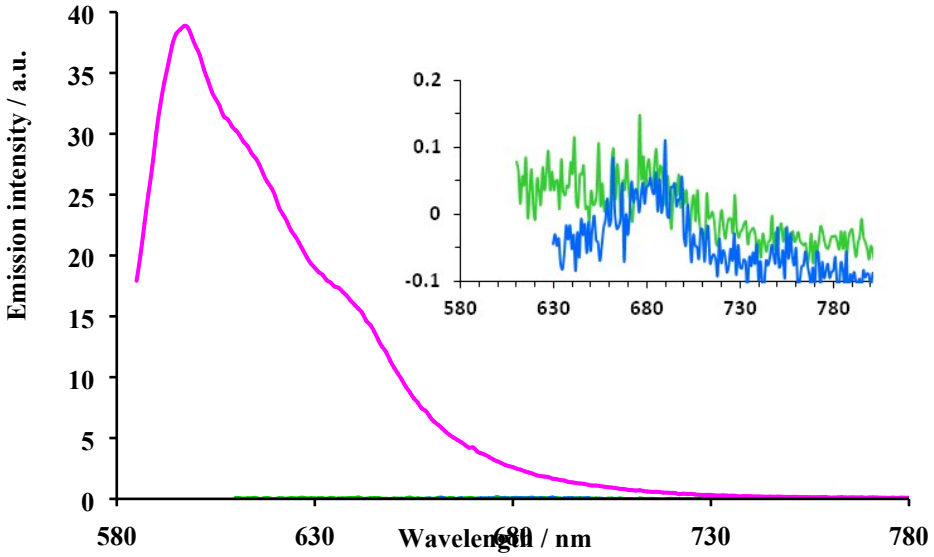

Figure S18. Emission spectra of **4** (pink, λ_{exc} = 600 nm), **1** (green, λ_{exc} = 580 nm), and **3** (blue, λ_{exc} = 620 nm) in toluene.

3. Electrochemical characterization of compounds 1 and 3

Table S1. Electrochemical oxidation and reduction of SubPcs **6**, **1**, and **3** – all values are in V vs Fc^{+}/Fc.

	E_{red3}	E_{red2}	E_{red1}	Eo_{x1}	Eo_{x2}	Eo_{x3}
1	-	–2.16	–1.54	0.12	0.69[a]	-
3	-	–2.10[a]	–1.63	0.03	0.15[b]	0.73[a]
6	–2.39	–2.05	–1.54	0.57	-	-

[a] Irreversible. [b] Strong adsorption.

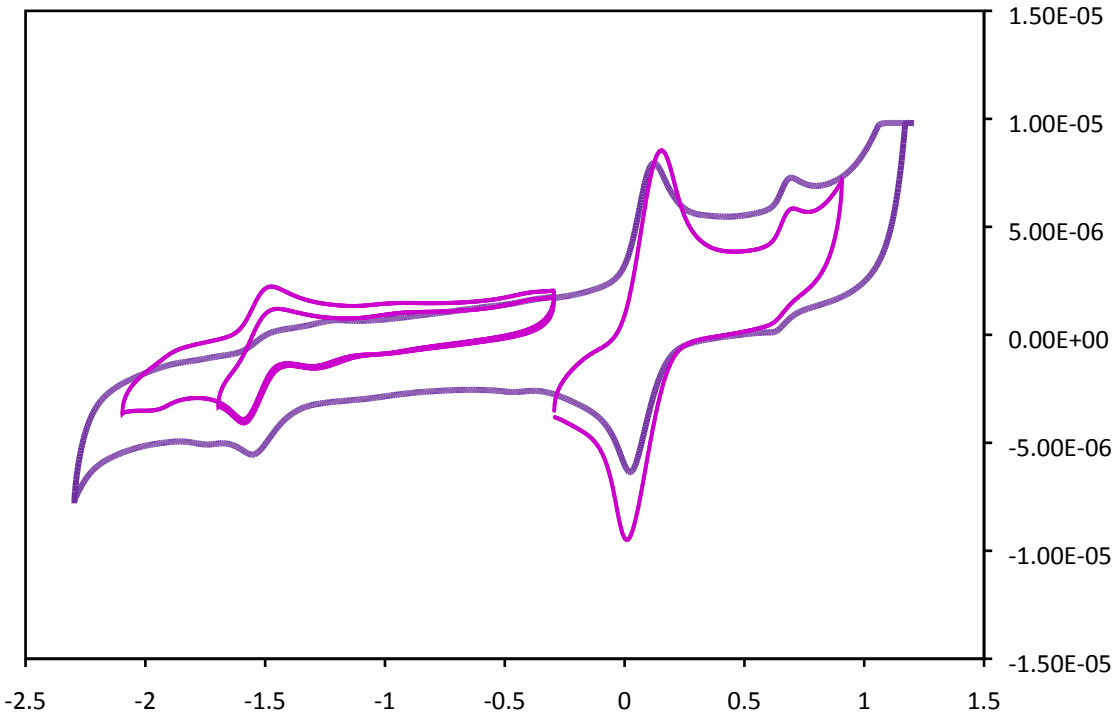

Figure S19. Cyclic voltammogram of Fc_3SubPc **1** (vs. Fc/Fc^+) in DCM

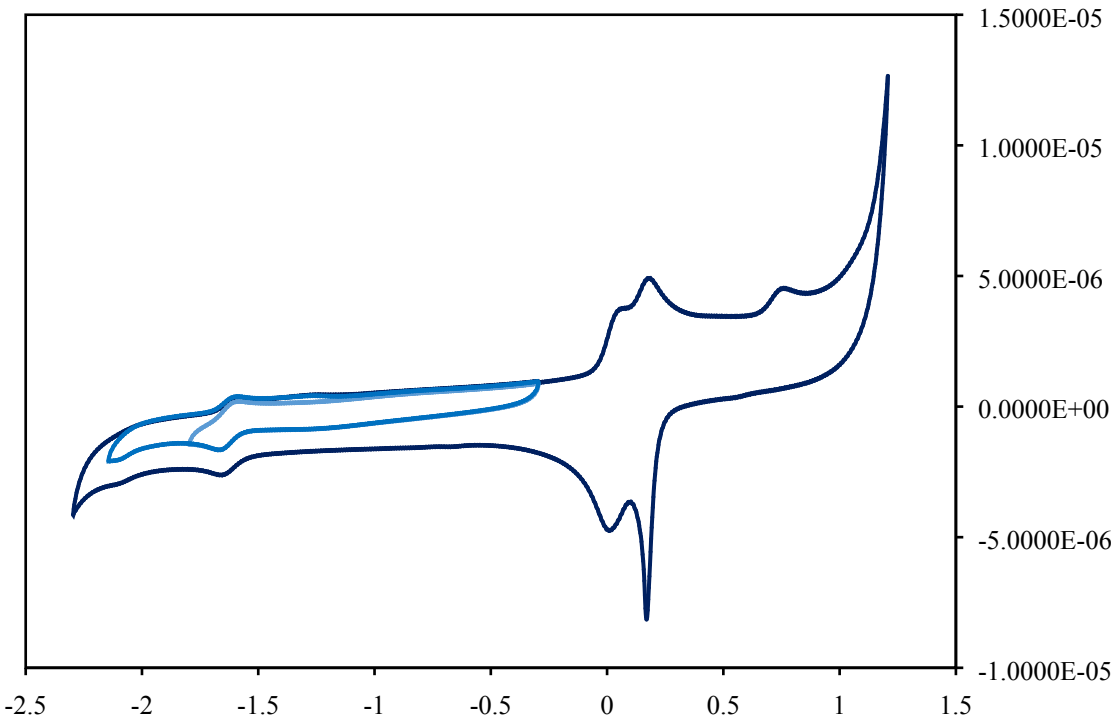

Figure S20. Cyclic voltammogram of compound Fc_6SubPc **3** (vs. Fc/Fc^+) in DCM

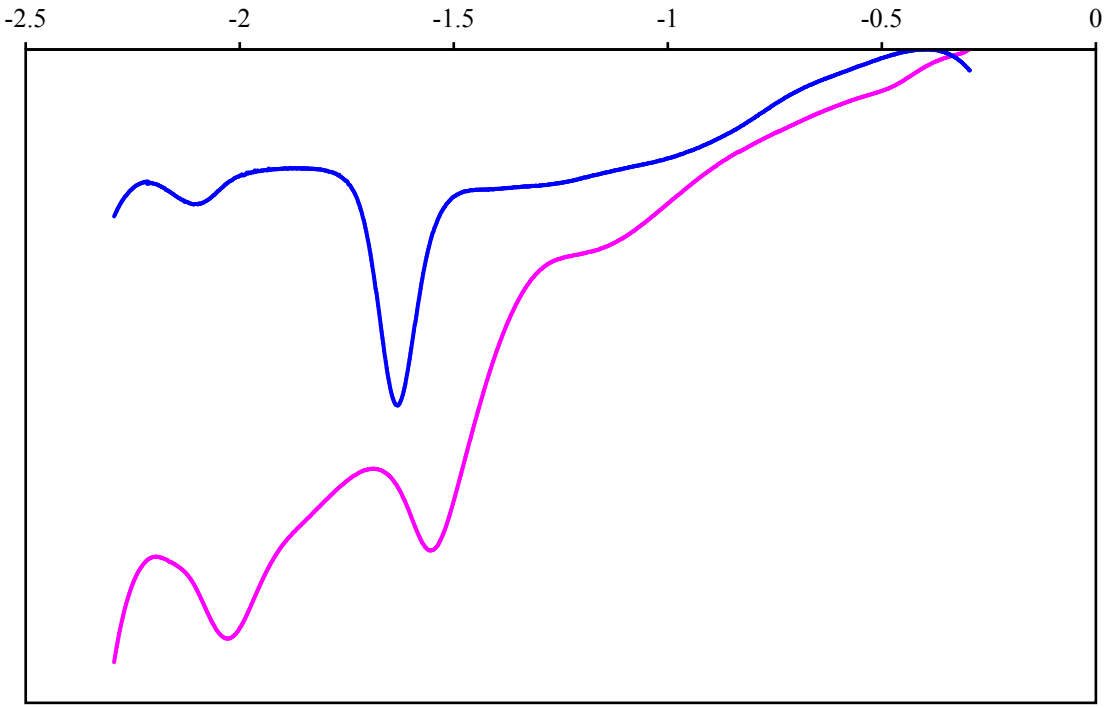

Figure S21. Square Wave Voltammetry plots (anodic window) of Fc_3SubPc **1** (pink) Fc_6SubPc **3**(blue) (vs. Fc/Fc^+) in DCM.

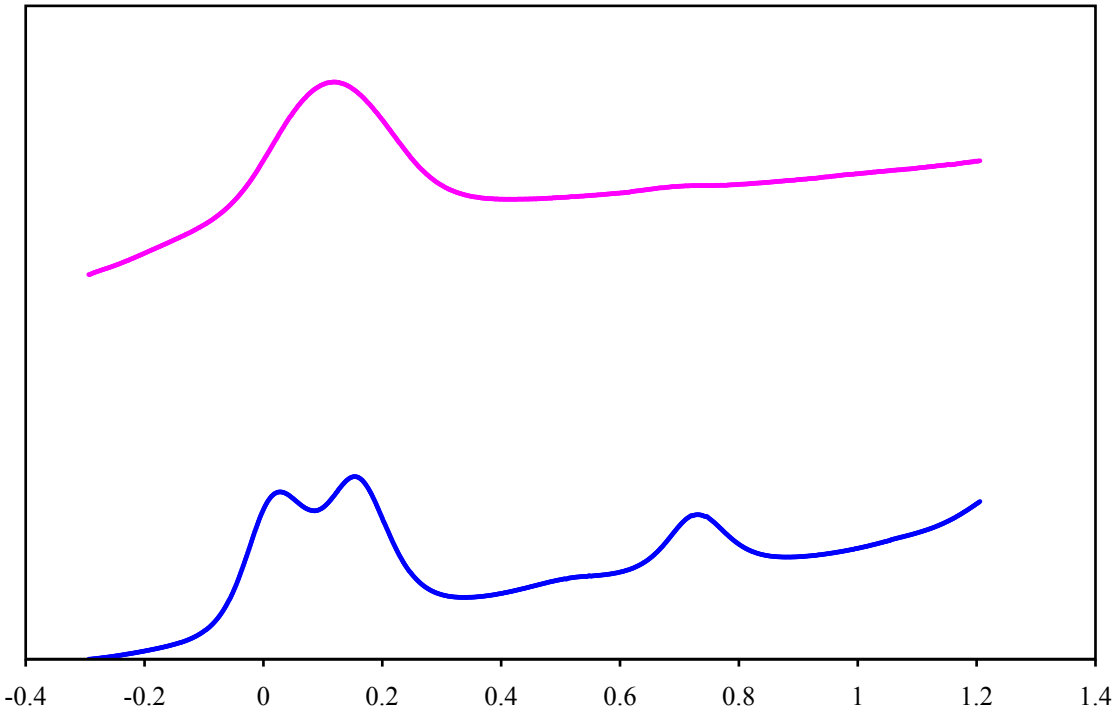

Figure S22. Square Wave Voltammetry plots (cathodic window) of Fc_3SubPc **1** (pink) Fc_6SubPc **3** (blue) (vs. Fc/Fc^+) in DCM.

Figure S23. Partial MO diagrams derived from B3LYP/6-31G (d,p)level DFT calculations of **1** (left) and **3** (right).

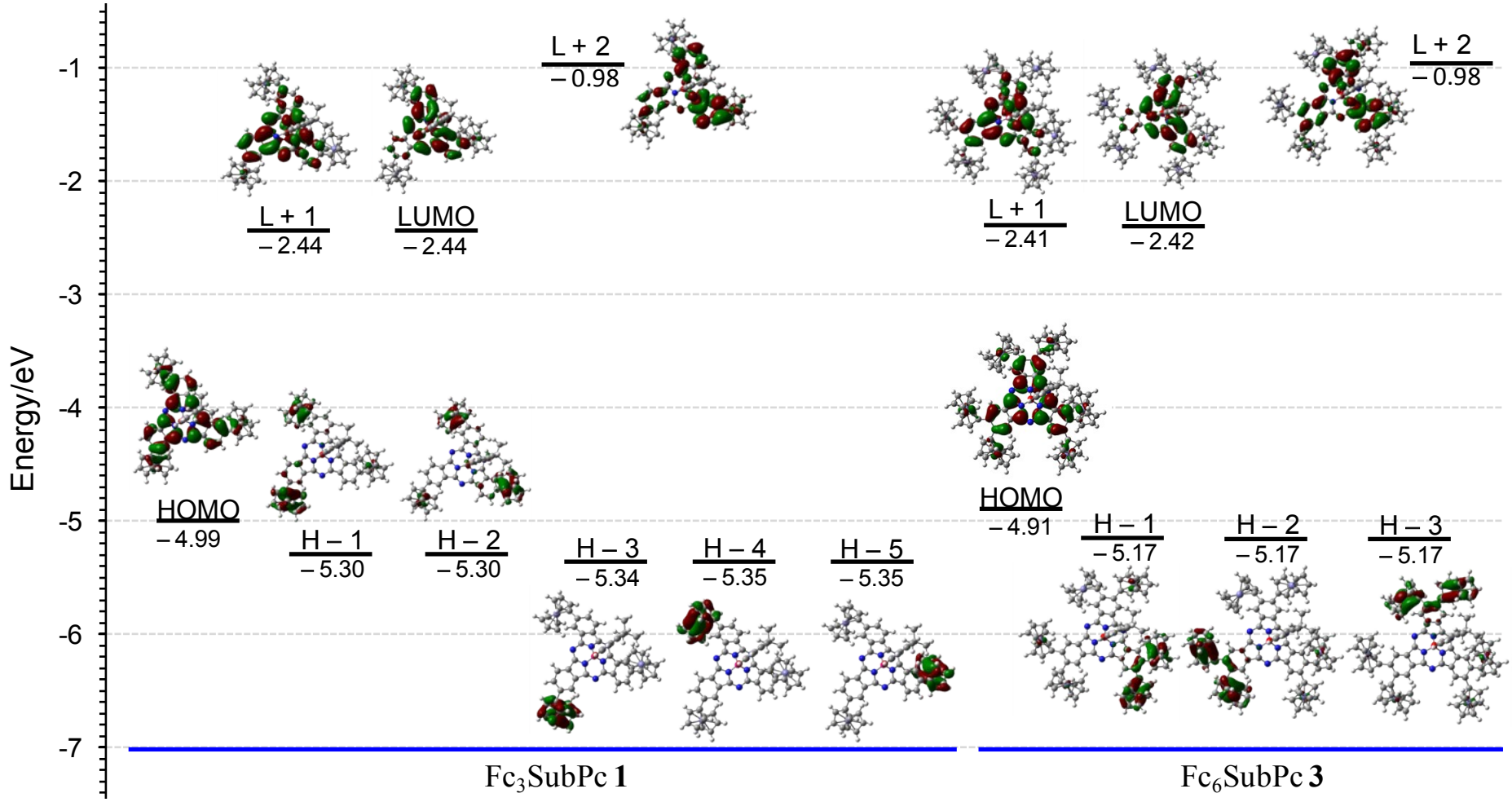

5. Transient Absorption Spectroscopy

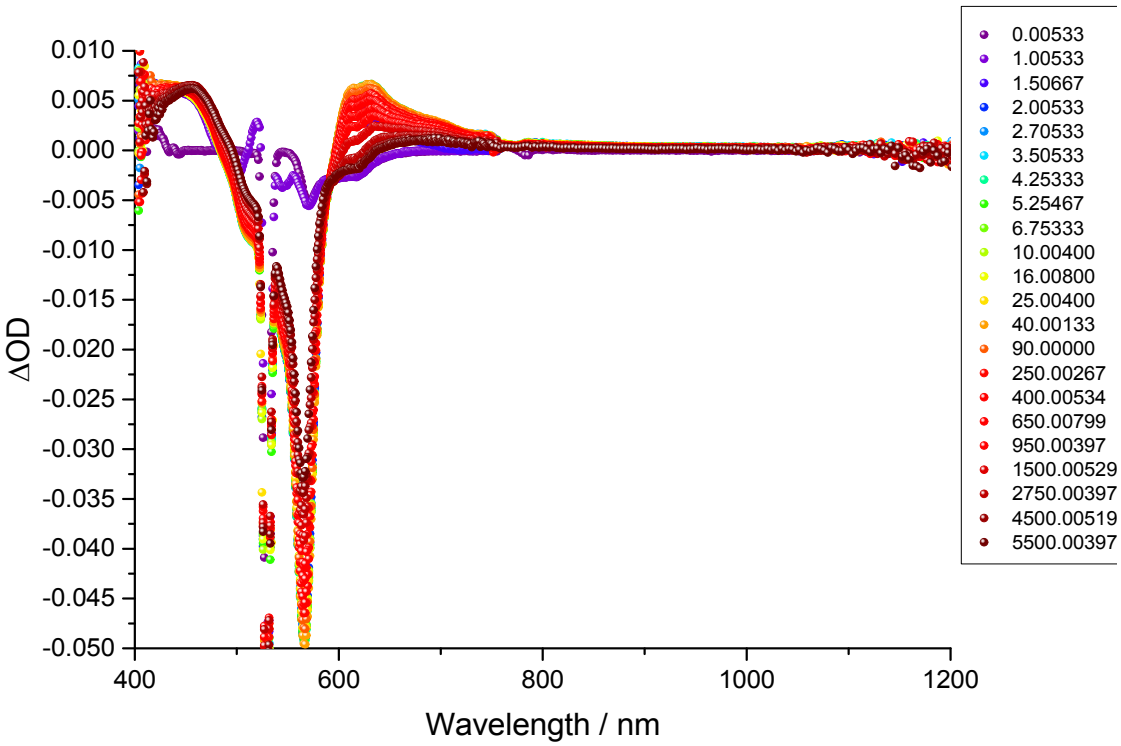

Figure S24. Transient absorption spectra of SubPc reference **6** in argon saturated chlorobenzene upon 530 nm photoexcitation.

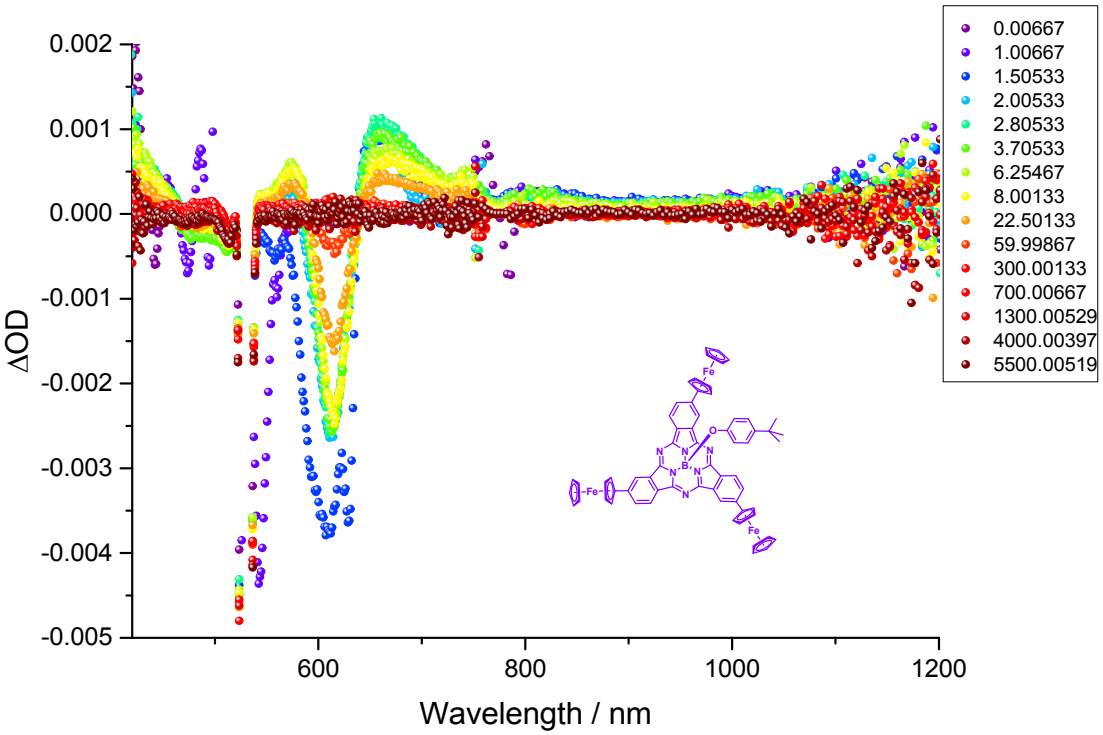

Figure S25. Transient absorption spectra of **1** in argon saturated chlorobenzene upon 530 nm photoexcitation.

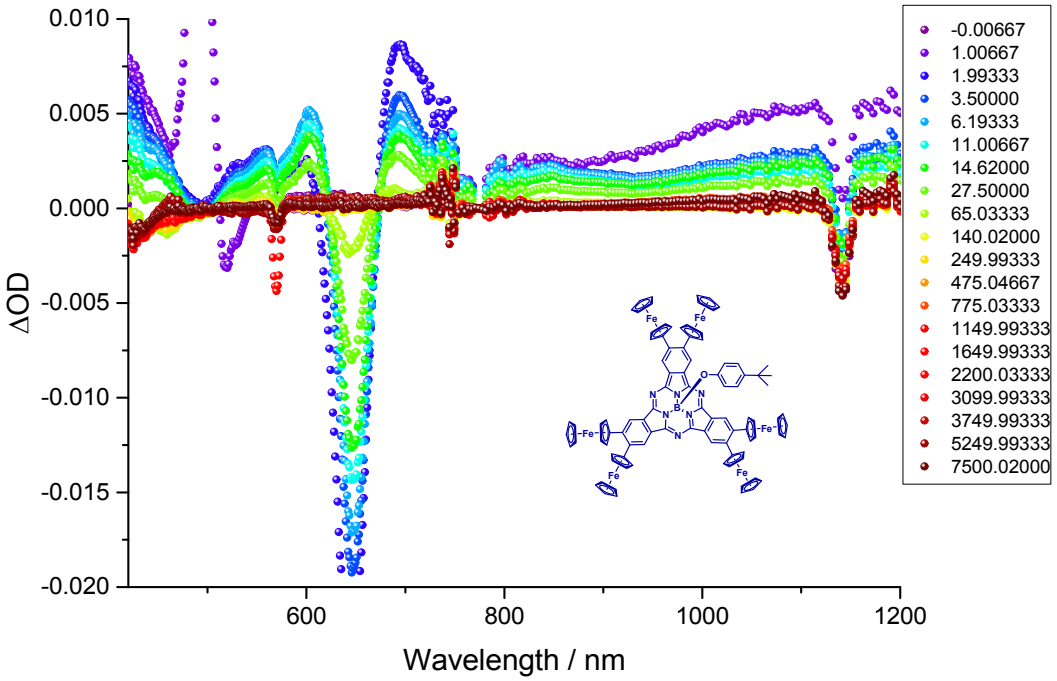

Figure S26. Transient absorption spectra of **3** in argon saturated chlorobenzene upon 568 nm photoexcitation.

6. Selected crystallographic data for 3•C_{60}

CCDC Deposit number 1531248

Crystals grew by vapor diffusion of hexanes into a toluene solution of the complex. A purple plate-like specimen of approximate dimensions 0.050 x 0.260 x 0.400 mm, was used for the X-ray crystallographic analysis.

Details of crystal data, data collection and structure refinement are listed in Tables S2 and S3. To minimise the expected disorder in the C_{60} molecule, the data collection was done at 200 K. As expected, C_{60} presents a high degree of disorder and had to be modelled applying geometrical constraints (mostly fitting pentagons as free rotating groups). Unfortunately, it was not possible to refine anisotropically the C_{60} molecule. Some disorder was also found in peripheral parts of the SubPc molecule, particularly in the Fe6 Fc substituent.

The structure displays large solvent accessible voids where highly disordered solvent molecules are located. The size of the accessible empty spaces in the unit cell has been estimated by PLATON SQUEEZE[v] to be of 1746 $Å^3$, containing a total electron count of 527 e^- not included in the final model. These values are in agreement with the presence of 10.5 highly disordered toluene molecules (525 e^-). If we also take into account the additional toluene molecule with half occupancy located in the asymmetric unit (that could be positioned in the final model using geometrical costraints), the total amount of interstitial solvent molecules in the crystal is 12.5 per unit cell, or 3.125 per asymmetric unit. Thus, the formula that can be inferred from the crystal structure is $C_{94}H_{73}BFe_6N_6O \cdot C_{60} \cdot 3.125\ C_7H_8$.

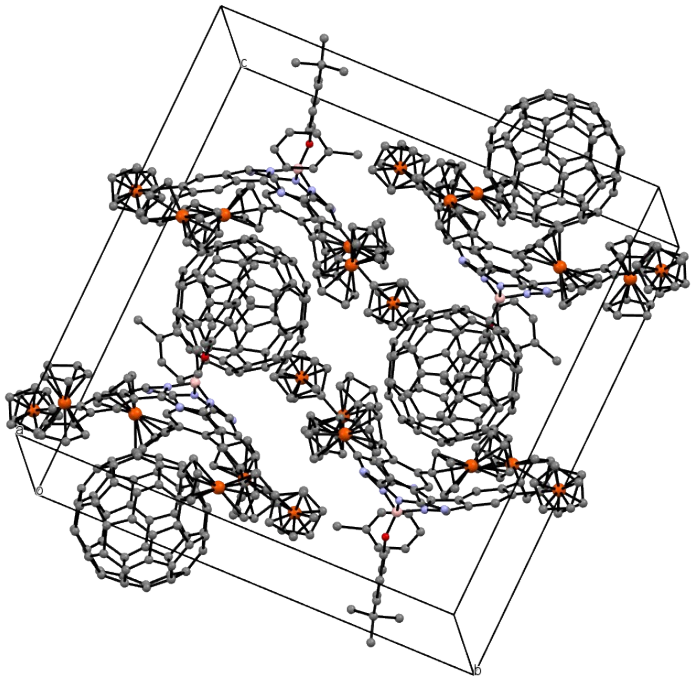

Figure S27. Unit cell and crystal packing of **3•C_{60}**

Table S2. Crystallographic data of **3**•C_{60}•3.125(toluene solvate)

Chemical formula	$C_{175.88}H_{98}BFe_6N_6O$	
Formula weight	2657.01 g/mol	
Temperature	200(2) K	
Wavelength	0.71073 Å	
Crystal size	0.050 x 0.260 x 0.400 mm	
Crystal system	monoclinic	
Space group	$P2_1/c$	
Unit cell dimensions	a = 18.502(1) Å	α = 90°
	b = 24.521(1) Å	β = 107.644(2)°
	c = 26.905(2) Å	γ = 90°
Volume	11632(1) Å^3	
Z	4	
Density (calculated)	1.517 g/cm^3	
Absorption coefficient	0.797 mm^{-1}	
F(000)	5457	

Table S3. Data collection and structure refinement for **3**•C_{60}•3.125(toluene solvate)

Theta range for data collection	1.15 to 25.35°	
Index ranges	-22<=h<=22, -29<=k<=29, -32<=l<=32	
Reflections collected	145221	
Independent reflections	21316 [R(int) = 0.0587]	
Absorption correction	multi-scan	
Max. and min. transmission	0.9610 and 0.7410	
Structure solution technique	direct methods	
Structure solution program	SHELXS-97 (Sheldrick 2008)	
Refinement method	Full-matrix least-squares on F^2	
Refinement program	SHELXL-2014 (Sheldrick 2014)	
Function minimized	$\Sigma\, w(F_o^2 - F_c^2)^2$	
Data / restraints / parameters	21316 / 1 / 1087	
Goodness-of-fit on F^2	1.035	
Δ/σ_{max}	0.001	
Final R indices	14038 data; I>2σ(I)	R_1 = 0.1581, wR_2 = 0.4650
	all data	R_1 = 0.1981, wR_2 = 0.5416
Weighting scheme	$w=1/[\sigma^2(F_o^2)+(0.5000P)^2]$ where $P=(F_o^2+2F_c^2)/3$	
Largest diff. peak and hole	6.232 and -1.849 eÅ^{-3}	
R.M.S. deviation from mean	0.261 eÅ^{-3}	

[i] Frisch, M. J.; Trucks, G. W.; Schlegel, H. B.; Scuseria, G. E.; Robb, M. A.; Cheeseman, J. R.; Scalmani, G.; Barone, V.; Mennucci, B.; Petersson, G. A.; Nakatsuji, H.; Caricato, M.; Li, X.; Hratchian, H. P.; Izmaylov, A. F.; Bloino, J.; Zheng, G.; Sonnenberg, J. L.; Hada, M.; Ehara, M.; Toyota, K.; Fukuda, R.; Hasegawa, J.; Ishida, M.; Nakajima, T.; Honda, Y.; Kitao, O.; Nakai, H.; Vreven, T.; Montgomery Jr., J. A.; Peralta, J. E.; Ogliaro, F.; Bearpark, M.; Heyd, J. J.; Brothers, E.; Kudin, K. N.; Staroverov, V. N.; Kobayashi, R.; Normand, J.; Raghavachari, K.; Rendell, A.; Burant, J. C.; Iyengar, S. S.; Tomasi, J.; Cossi, M.; Rega, N.; Millam, J. M.; Klene, M.; Knox, J. E.; Cross, J. B.; Bakken, V.; Adamo, C.; Jaramillo, J.; Gomperts, R.; Stratmann, R. E.; Yazyev, O.; Austin, A. J.; Cammi, R.; Pomelli, C.; Ochterski, J. W.; Martin, R. L.; Morokuma, K.; Zakrzewski, V. G.; Voth, G. A.; Salvador, P.; Dannenberg, J. J.; Dapprich, S.; Daniels, A. D.; Farkas, O.; Foresman, J. B.; Ortiz, J. V.; Cioslowski, J.;Fox, D. J. Gaussian 09, Revision A.02, Gaussian, Inc., Wallingford CT, 2009.

[ii] Claessens, C. G.; Vicente-Arana, M. J.; Torres, T. *Chem. Commun*., **2008**, 6378–6380.

[iii] Sharman, W. M.; van Lier, J. E. *J. Porphyrins Phthalocyanines*, **2005**, *9*, 651.

[iv] Sugimoto, H.; Tanaka T.; Osuka, A. *Chem. Lett.* ***2011,*** 40*, 629.*

[v] Spek, A. L., *Acta Cryst*, **2015**, C71, 9-18.